JPEDAV (2010) 31:327–332
DOI: 10.1007/s11669-010-9710-z
1547-7037 ©ASM International

Investigation of the Phase Relations in the Al-Rich Alloys of the Al-Sc-Hf System in Solid State

L.L. Rokhlin, N.R. Bochvar, J. Boselli, and T.V. Dobatkina

(Submitted January 18, 2010; in revised form March 2, 2010)

Using electrical resistivity measurements, optical microscopy, and scanning electron microscopy (SEM) with energy dispersive x-ray analysis (EDS), the combined solubility of Sc and Hf in solid Al and the phases in equilibrium with Al solid solution at 600, 500, and 400 °C were studied. The investigation indicated the progressive decrease of the total solubility of Sc and Hf in solid Al with increasing Sc/Hf ratio in the alloys and decreasing temperature. $ScAl_3$ and $HfAl_3$ were observed in equilibrium with Al without formation of a continuous solid solution between them. Based on the established extension of the Al solid solution and also extensions of the $ScAl_3$ + (Al) and $HfAl_3$ + (Al) phase fields, the partial isothermal section of the Al-Sc-Hf phase diagram at 600 °C was constructed.

Keywords aluminum alloys, phase diagram, phase equilibria, solid solution, ternary phase diagram

1. Introduction

There appears to be no information in the literature regarding the Al-rich part of the Al-Sc-Hf ternary phase diagram. This phase diagram is interesting because Sc and Hf interact similarly with Al in the binary systems. The most interesting part of the Al-Sc-Hf phase diagram is the Al-rich corner, because Sc is known to improve significantly the strength of aluminum alloys.[1-3] In this work, the Al-rich part of the Al-Sc-Hf phase diagram was studied.

1.1 Adjoining Binary Systems

The Al-rich side of the binary phase diagram Al-Sc has been studied extensively. According to Massalski et al.,[4] the main features are the invariant eutectic reaction at 655 °C near the melting point of Al (660.452 °C), the small solubility of Sc in solid Al, which decreases with decreasing temperature from ~0.24 at.% at 655 °C to ~0.03 at.% at 500 °C and the existence of the compound $ScAl_3$ in equilibrium with solid Al. The crystal structure of the $ScAl_3$ is cubic of the $L1_2$ type (Au_3Cu prototype, Pearson symbol *cP*4). The Al-Hf phase diagram is characterized, according to our previous work,[5] by the peritectic invariant reaction at 661 °C and low solubility of Hf in solid Al, which decreases with decreasing temperature from 0.153 at.% at 661 °C to 0.05 at.% at 500 °C. The composition of the phase in equilibrium with Al solid solution in the Al-Hf system was confirmed to be $HfAl_3$.[5] Two allotropic forms have been reported for this compound, with crystal structures described by the Pearson symbols *tI*8 (prototype $TiAl_3$) and *tI*16 (prototype $ZrAl_3$).[4]

2. Methods

2.1 Preparation of the Alloys

The alloys for investigation of the combined solubility of Sc and Hf in solid Al were prepared by melting in an electrical resistance furnace in crucibles of sintered Al_2O_3. In order to improve the joining of Al pieces during melting, small amounts of the Russian Standard flux VI2 containing 38-46%[1] $MgCl_2$, 32-40% KCl, 3-5% CaF_2, 5-8% $BaCl_2$, 1.5% MgO, and <8% (NaCl + $CaCl_2$) was added. Aluminum (99.99%), Sc (99.875%), and Hf (99.8%) were used as the starter materials. Sc and Hf were added into the Al melt in the form of the master alloys Al-0.8% Sc, Al-4.2% Sc, Al-11% Hf, and Al-2.44% Hf prepared using Al, Sc, and Hf of similar purity. The master alloys were melted under purified Ar in an arc furnace equipped with non-consumable W electrode and water-cooled Cu hearth. The alloy melts were poured into stainless steel molds in order to obtain cylindrical ingots of about 15 mm in diameter and 90 mm in length.

These ingots were first worked by rolling to the rods to a square cross-section of 8 by 8 mm^2. The preliminary cold working of the ingots to rods was conducted to accelerate diffusion processes in the alloys during annealing. The reduction in area amounted to about 50%. The rods were cut into pieces and annealed at 600, 500, and 400 °C to reach the equilibrium state at these temperatures. The annealing was conducted by applying the following steps in succession: 600 °C for 30 h, 500 °C for 100 h, and 400 °C for 100 h. After annealing, the samples were quenched into

L.L. Rokhlin, N.R. Bochvar, and **T.V. Dobatkina**, Baikov Institute of Metallurgy and Materials Science RAS, Moscow, Russia; **J. Boselli**, Alcoa Technical Center, Alcoa Center, Pittsburgh PA, USA. Contact e-mail: rokhlin@ultra.imet.ac.ru.

[1]Here and further wt.% unless noted differently.

water at room temperature. The chosen annealing durations at every temperature were considered to be sufficient to reach equilibrium state based on the preceding works where the binary Al-Sc and Al-Hf phase diagrams were studied. The heat treated samples were used for determination of the Al solid solution boundaries at the quenching temperatures by the electrical resistivity method and microstructural observations.

Separate alloys were cast for identification of the phases in equilibrium with Al solid solution. They contained 5%(Sc + Hf) at different Sc/Hf ratios amounting up to 3.06 at.% Sc and up to 0.79 at.% Hf. These alloys were prepared by melting in the arc furnace to obtain 20 mm ingots in diameter and 10 mm in height.

2.2 Investigation Techniques

The compositions of all ingots were checked by atom-emission spectroscopy using induction plasma. The equipment used was the Inductivity Coupled Plasma-Atomic Spectrometer of ULTIMA 2C, Jobin-Yvon Firm. The reported compositions of the alloys are based on the chemical analysis.

The microstructure of the alloys was studied using optical microscopy and the scanning electron microscope (SEM). For the optical microscopy observations, the alloy samples were prepared by grinding on successively finer abrasive papers. After grinding, the samples were polished by electrolysis in solution consisting of H_2SO_4—100 mL, H_3PO_4—400 mL, Cr_2O_3—50 g, H_2O—25 mL at a temperature of 70-90 °C and electrical current density of 0.7-0.9 A/dm^2. Simultaneously, the samples were etched. For the optical microscopy observations, the Neophot 2 microscope (VEB Carl Zeiss, Jena, Germany) was used at various magnifications. For scanning electron microscopy, the LEO-430i scanning electron microscope equipped with a LINK-ISIS-300 energy-dispersive x-ray analyzer was used. Compositions of Al solid solution and inclusions in the alloy structures were assessed by local x-ray spectral analysis (EDS). Samples for the SEM investigation were prepared the same way as for the optical microscopy observations.

In the experiments, electrical resistivity measurements were used, which were performed by the compensative method with Russian low-ohm potentiometer R348. Error of the electrical resistivity measurements was estimated to be ±0.7%.

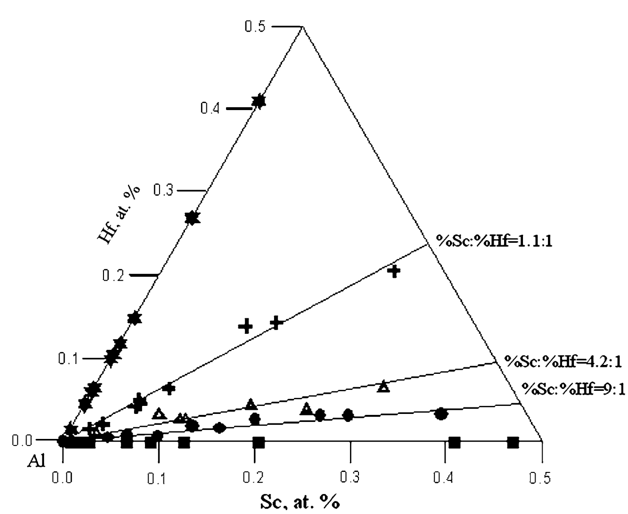

Fig. 1 Selected alloys for investigation of the Sc and Hf solubility in solid Al in the ternary Al-Sc-Hf system

3. Results

3.1 Combined Solubility of Sc and Hf in Al Solid Solution

Taking into account the small solubility of Sc and Hf in solid Al in the binary systems, small solubilities in the ternary Al-Sc-Hf system could be anticipated. For this case, electrical resistivity measurement was considered to be the most reliable method for determination of the solid solution boundaries and, therefore, it was chosen as the main method for estimation of the combined solubility of Sc and Hf in solid Al in the ternary Al-Sc-Hf system. The planned compositions of the alloys for determination of the solubility limits of Sc and Hf in the ternary system were disposed along the sections running from the Al corner with Sc/Hf ratios being equal to 3:1, 1:1, and 1:3 in wt.%. Binary Al-Sc and Al-Hf alloys were investigated simultaneously. Compositions of the ternary alloys are indicated on the concentration triangle in Fig. 1 in at.%. As one can see, they correspond well to three sections with constant Sc/Hf ratios equal to 9:1, 4.2:1, and 1.1:1 in at.%.

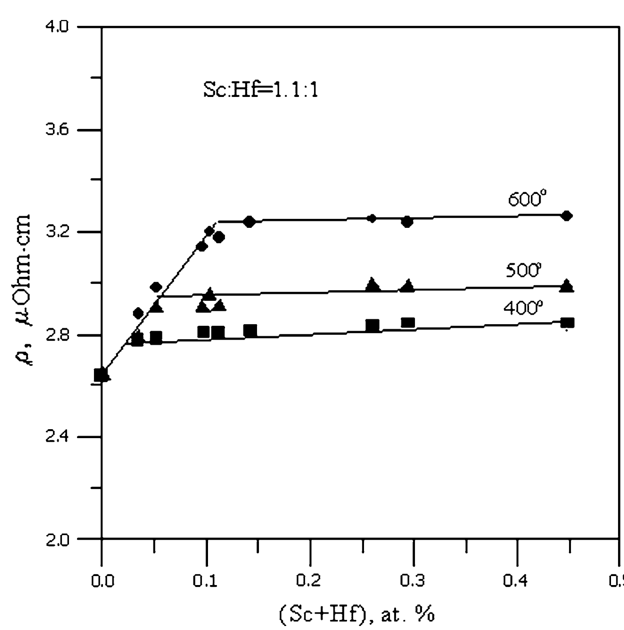

Fig. 2 Electrical resistivity (ρ) of the Al-Sc-Hf alloys for a Sc/Hf ratio of 1.1:1 (in at.%) vs. the (Sc + Hf) content for different annealing temperatures

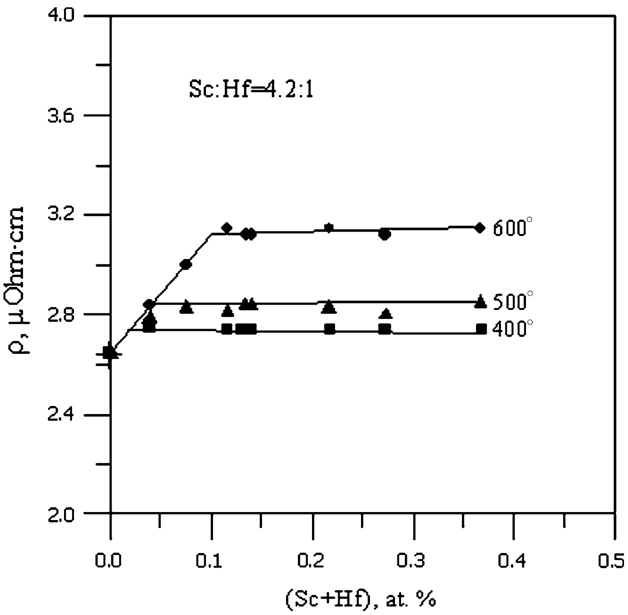

Fig. 3 Electrical resistivity (ρ) of the Al-Sc-Hf alloys for a Sc/Hf ratio of 4.2:1 (in at.%) vs. the (Sc + Hf) content for different annealing temperatures

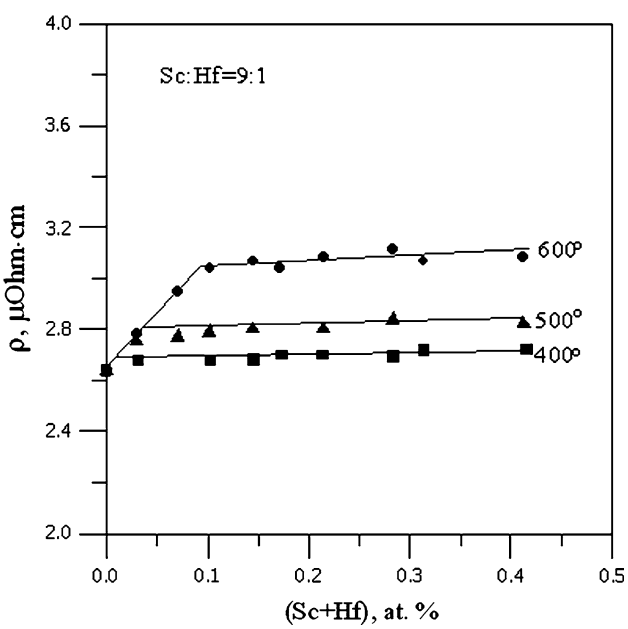

Fig. 4 Electrical resistivity (ρ) of the Al-Sc-Hf alloys for a Sc/Hf ratio of 9:1 (in at.%) vs. the (Sc + Hf) content for different annealing temperatures

The electrical resistivity curves are presented in Fig. 2, 3, 4. They indicate electrical resistivity changes with increasing Sc and Hf contents and their sum in the alloys. The curves demonstrate clear slope changes corresponding to the total solubility of Sc and Hf at given annealing temperatures. The positions of the slope changes show that the total solubility of Sc and Hf in solid Al decreases with decreasing

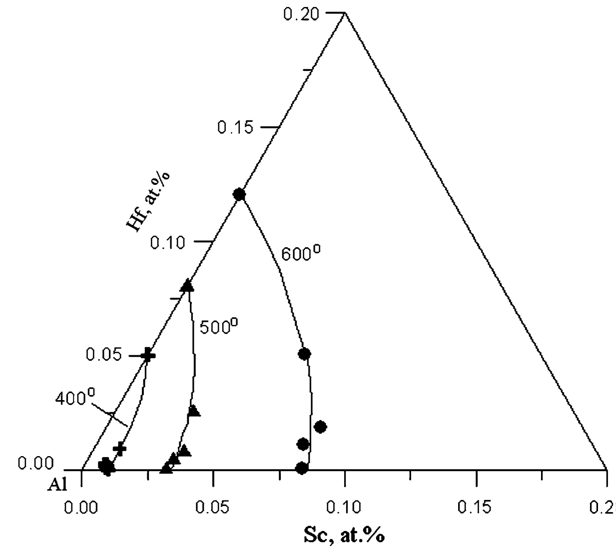

Fig. 5 Al solid solution fields in the Al-Sc-Hf phase diagram at 600, 500, and 400 °C

temperature. The Al solid solution fields at 600, 500, and 400 °C constructed by using these data are shown in Fig. 5. They show, along with contraction of the single phase field with lowering temperature, the progressive decrease of the Sc and Hf solubility in solid Al with increasing Sc/Hf ratio. The form of the Al solid solution field shows a gradual decrease of solubility of each transition metal with increasing content of the other. Decrease of the Sc solubility in solid Al with increasing Hf content is insignificant at small Hf content, but becomes more pronounced at higher Hf. The Sc solubility values in the binary Al-Sc system obtained in this work agree with those published in Ref 6, 7.

3.2 Investigation of Microstructure

Observation of the as-cast Al-Sc-Hf alloys with higher contents of Sc (up to 3.1 at.%) and Hf (up to 0.79 at.%) under optical microscopy revealed the presence of coarse gray crystals of compounds containing Sc and/or Hf in equilibrium with Al solid solution. The gray crystals of $ScAl_3$ in the binary Al-Sc alloys were typically of equiaxed form with rounded edges (Fig. 6a), whereas the gray crystals of $HfAl_3$ in the binary Al-Hf alloys were typically of elongated form with more rugged edges (Fig. 6b). Both types of crystals demonstrated some dendritic character. In the ternary Al-Sc-Hf alloys with higher contents of Sc, the form of the gray crystals was similar to that in the binary Al-Sc alloys, and in the ternary alloys with high contents of Hf the form of the gray crystals was similar to that in the binary Al-Hf alloys (Fig. 6b). In the latter alloys, both types of phases could be observed simultaneously.

The SEM study of the Al-Sc-Hf alloys along the section between Al-3.06 at.% Sc and Al-0.79 at.% Hf revealed crystals having the same morphology as those observed via optical microscopy. The typical micrographs with the compound crystals are presented in Fig. 7. In Table 1 the results of the EDS analysis of the compounds are

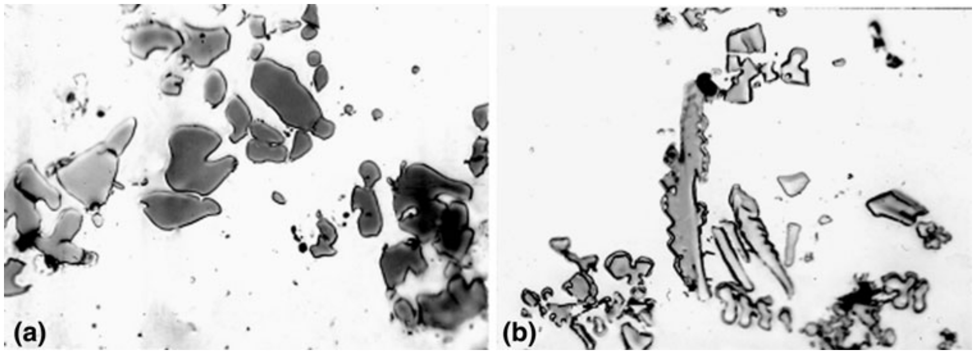

Fig. 6 Microstructure of the Al-Hf-Sc alloys annealed at 600 °C, ×630. (a) Al-3.06at.%Sc, (b) Al-1.55at.%Sc-0.39at.%Hf

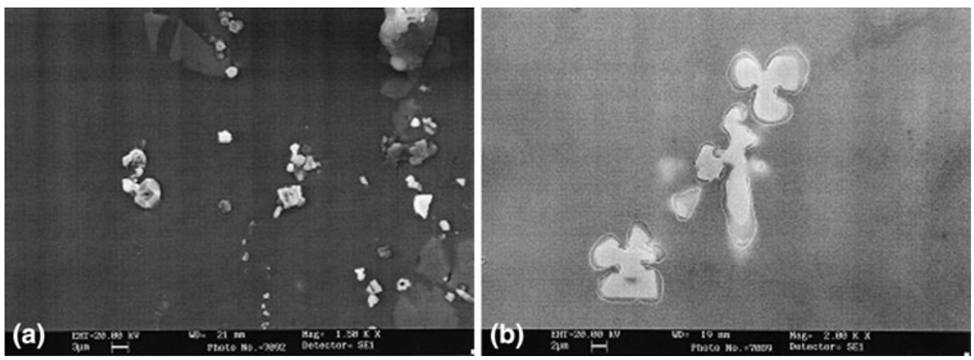

Fig. 7 Microstructure of the Al-Sc-Hf alloys annealed at 600 °C in SEM. (a) Al-0.93at.%Sc-0.55at.%Hf, (b) Al-1.55at.%Sc-0.39at.%Hf

Table 1 Results of the EDS analysis of the compound crystals in the Al-Sc-Hf alloys along the section between Al-3.06at.%Sc and Al-0.79at.%Hf

	Composition of the crystals, mass%			Composition of the crystals, at.%			
Alloy	**Al**	**Sc**	**Hf**	**Al**	**Sc**	**Hf**	**Phase**
Al-3.06at.%Sc	61.48	35.24	3.28*	73.96	25.44	0.60*	$ScAl_3$
	63.43	37.03	−0.46*	74.11	25.97	−0.08*	$ScAl_3$
	63.86	33.51	2.63*	75.69	23.84	0.47*	$ScAl_3$
Al-0.79at.%Hf	29.58	−0.04*	70.46	73.57	−0.06*	26.49	$HfAl_3$
	35.11	−0.08*	64.97	78.22	−0.10*	21.88	$HfAl_3$
Al-1.85at.%Sc-0.31at.%Hf	51.54	22.08	26.37	74.94	19.27	5.80	($ScAl_3$)
Al-1.55at.%Sc-0.39at.%Hf	50.55	20.99	28.46	74.94	18.68	6.38	($ScAl_3$) core
	60.76	24.57	14.67	78.17	18.97	2.85	($ScAl_3$)
	53.28	23.98	22.74	74.93	20.24	4.83	rim
	56.75	25.45	17.81	75.95	20.44	3.60	
Al-0.93at.%Sc-0.55at.%Hf	45.84	17.31	36.84	74.18	16.81	9.01	($ScAl_3$)
Al-0.62at.%Sc-0.63at.%Hf	40.10	7.32	52.57	76.47	8.38	15.15	($HfAl_3$)
	36.94	7.45	55.61	74.15	8.98	16.88	($HfAl_3$)
	36.83	6.82	56.35	74.49	8.28	17.23	($HfAl_3$)

*In limits of error

summarized. In the SEM study two types of compound crystals were distinguished. Crystals of one type were enriched in Sc and they can be recognized as the $ScAl_3$-base solid solution containing Hf (or without Hf in the binary Al-Sc alloy). Crystals of the second type were enriched in Hf and they can be recognized as the $HfAl_3$-base solid solution containing Sc (or without Sc in the binary Al-Hf alloy). The crystals of both types were distinguished also by

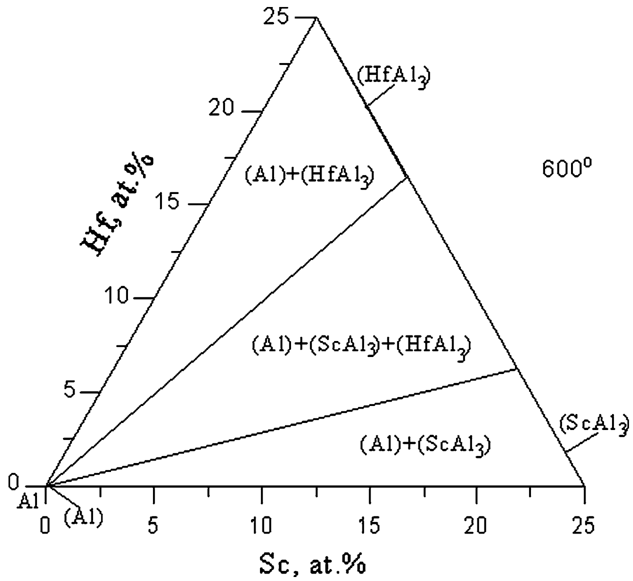

Fig. 8 Partial isothermal section of the Al-Sc-Hf phase diagram at 600 °C

brightness. The crystals enriched by Hf were lighter than the crystals enriched by Sc because of the higher atomic number of Hf, as compared with that of Sc. Both types of crystals can be seen together in Fig. 7(a). In this alloy, only dark crystals were analyzed because of the small size of the light crystals. In Fig. 7(b) the crystals with the $ScAl_3$ morphology are shown to have a light core and dark rim. The EDS analysis indicated higher Hf content in the core, as compared with the rim. This is attributed to the kinetics of crystal formation under non-equilibrium conditions during solidification.

In all alloys, EDS analysis of the 2nd phases indicated Al contents of about 75 at.%. Therefore, in the $ScAl_3$-base solid solution, Hf substitutes for Sc, and in the $HfAl_3$-base solid solution Sc substitutes for Hf. In Table 1 the $ScAl_3$-base solid solution is designated by ($ScAl_3$), and the $HfAl_3$-base solid solution is designated by ($HfAl_3$). The limit of the Hf content in the $ScAl_3$-base solid solution was found to be about 8.7 at.% Hf (36 mass% Hf) according to the EDS analysis in the alloy Al-0.93at.%Sc-0.55at.%Hf, after accounting for a small correction assuming that the sum of the Sc and Hf contents in the compound must be 25 at.%. The limit of the Sc content in the $HfAl_3$-base solid solution was found to be 8.6 at.% Sc (7.2 mass% Sc) according to the EDS analysis of the crystals in the alloy Al-0.62at.%Sc-0.63at.%Hf, after correcting so that the sum of (Sc + Hf) is equal to 25 at.%.

Absence of continuous complete solid solution between $ScAl_3$ and $HfAl_3$ could be expected because of the different nature of the crystal structures of these compounds.

3.3 Partial 600 °C Isothermal Section

Based on the results of the SEM investigation of the phases in equilibrium with Al together with data on extension of the Al solid solution field, the partial isothermal section of the Al-Sc-Hf phase diagram at 600 °C was constructed. The section is presented in Fig. 8. The partial isothermal sections at 500 and 400 °C are similar in nature.

4. Discussion

The described investigation of the Al-Sc-Hf phase diagram in the Al corner revealed its important feature, which can be considered as typical one for the phase diagrams of the aluminum alloys with the transition earth metals. It is the small solubility of the transition metals in solid Al. Such a small solubility in solid Al exists, for example in the Al-Cr, Al-Zr, and Al-Mn systems.[4] The values of the transition metal solubility in solid Al are especially small, if they are estimated in atomic percent, but not in weight ones. Despite of the small combined solubility of Sc and Hf in solid Al, the experiments indicated clearly the solubility decrease with lowering temperature. This fact suggests a possibility of the supersaturated Al solid solution formation in the Al alloys containing Sc and Hf and its decomposition during heat treatment resulting in the certain effect on the properties of the alloys.

5. Conclusions

1. The combined solubility of Sc and Hf in solid Al was determined at 600, 500, and 400 °C. Experiments indicate contraction of the Al solid solution field in the Al-Sc-Hf phase diagram with decreasing temperature. Sc and Hf were shown to decrease the solubility of each other in solid Al. The total solubility of Sc + Hf in solid Al decreases gradually with increasing Sc/Hf ratio in the alloys.
2. Only the $ScAl_3$ and $HfAl_3$ phases of the respective binary systems exist in equilibrium with Al solid solution. The phase $ScAl_3$ can dissolve Hf, and the phase $HfAl_3$ can dissolve Sc.
3. The partial isothermal section of the Al-Sc-Hf phase diagram at 600 °C in the Al corner to 25 at.% (Sc + Hf) has been constructed.

Acknowledgments

The investigation was supported by the Alcoa Technical Center, contract No. 400054987. The authors would like to thank Dr. J. Murray for her review of this paper.

References

1. M.E. Drits, N.I. Turkina, E.S. Kadaner, and T.V. Dobatkina, *Redkie metally v tsvetnykh splavakh (Rare Metals in Non-Ferrous Alloys)*, "Nauka", Moscow, 1975, p 160-167
2. M.E. Drits, L.S. Toropova, Yu.G. Bykov, V.I. Elagin, and Yu.A. Filatov, *Metallurgiya I metallovedenie tsvetnykh splavov (Metallurgy and Metals Science of Non-Ferrous Alloys)*, "Nauka", Moscow, 1982, p 213-223, in Russian

3. R.R. Sawtell and C.L. Jensen, Mechanical Properties and Microstructures of Al-Mg-Sc Alloys, *Metall. Trans. A*, 1990, **21A**(2), p 421-430
4. *Binary Phase Diagrams*, 2nd edn., T.B. Massalski (Editor-in-chief), ASM International, Materials Park, OH, 1990
5. L.L. Rokhlin, N.R. Bochvar, T.V. Dobatkina, and V.L. Leontyev, Investigation of the Al-Rich Part of the Al-Hf Phase Diagram, *Metally*, 2009, (3), p 93-98, in Russian
6. M.E. Drits, E.S. Kadaner, T.V. Dobatkina, and N.I. Turkina, About Character of the Interaction between Scandium and Aluminum in the Aluminum-Rich Part of the Al-Sc System, *Izvestiya of Akademii Nauk SSSR, Metally (News of the Academy of Sciences of USSR, Metals)*, 1973, (4), p 213-217
7. S.J. Fujikawa, M. Sugaya, H. Takei, and K.J. Hirano, Solid Solubility and Residual Resistivity of Scandium in Aluminium, *J. Less-Common Met.*, 1979, **63**(1), p 87-97